Diffusion Coefficients in Swelling Polypyrrole: ESCR and Cottrell Models†

Iván J. Suárez,‡ Toribio F. Otero,* and Manuel Márquez§

Laboratory of Electrochemistry Intelligents Materials and Devices (CEMI), Ingenieros Industriales, Campus Alfonso XIII, Universidad Politécnica de Cartagena, 30203 Cartagena, Murcia, Spain

Received: September 1, 2004; In Final Form: November 19, 2004

Reliable diffusion coefficients, *D*, for the diffusion of perchlorate anions into polypyrrole films during polymeric oxidation were obtained from chronoamperometric results. Two different models were used to calculate *D*: the Cottrell equation and the electrochemically stimulated conformational relaxation (ESCR) model. As expected, the initial Cottrell hypothesis was far from swelling/shrinking polymeric electrodes and the obtained *D* range was from 10^{-10} to 10^{-6} cm^2 s^{-1}. The ESCR model, based on the internal diffusion that takes place from regions where the steady state of oxidation has already been reached to regions where the oxidation is only just beginning, provided values of *D* ranging from 0.4×10^{-9} to 2.2×10^{-9} cm^2 s^{-1}, which is close to the values expected for a gel. When a constant amplitude is kept for the potential step, *D* increases with increasing initial anodic potentials, i.e., from increasingly swollen films. When it is stepped to the same oxidation potential, *D* decreases when starting from more cathodic potentials, i.e., from a more compact structure. These changes in *D* can be attributed to (i) swelling processes during oxidation, giving a gel-like structure; (ii) compacting processes at increasing cathodic potentials; (iii) the increasing thickness of the film during oxidation; and (iv) a decrease in film viscosity during the swelling process.

Introduction

Conducting polymers have been attracting increasing interest for more than 25 years because of the reverse changes of several orders of magnitude that two of their properties undergo during reverse electrochemical oxidation and reduction processes: conductivity and composition[1] (the last due to the nonstoichiometric nature[2] of the oxidized material). Linked to the reverse change in material composition, several other properties can be controlled in a reversible way by means of the electrochemical reaction: volume, color, stored charge, porosity, electron/ion transduction, medical dosage, and so forth. All the devices (artificial muscles, smart windows, polymeric batteries, artificial glands, electron/ion transducers) related to these properties work either under the diffusion kinetic control of the counterions required for charge balance or under slower relaxation kinetic control of the conformational structure. The best way to design the most suitable practical kinetic conditions for the different devices is to find a reliable and fast method for determining diffusion coefficients inside the constituent polymer.

Different techniques, such as chronoamperometric methods (by means of the Cottrell model)[3] or electrochemical impedance, have been used to measure ion diffusion. In impedance measurements, discrimination between electronic transport (high-frequency measurements) and ionic transport (low-frequency measurement) can be expected,[4] and any conducting polymer can be studied under different oxidation states.[5−7] The selection of an equivalent circuit, which is necessary to determine the diffusion coefficient (*D*), implies the selection of a physical model: fixing the edge condition to avoid a porous structure,[8] considering the porous nature of the oxidized polymer,[9] combining the impedance measurements with the Nernst−Einstein equation,[10] or comparing the *D* obtained by simulating a porous structure with the Cottrell model.[11] The high values of *D* obtained with the Cottrell model have been attributed to its exclusion of migrational contributions,[11] while the weak point of the impedance method is the a posteriori requirement of a physical model in order to select the suitable equivalent circuit, each scientist having his/her own preference.

Ion transport has also been monitored in open circuits after application of a current step and following the potential relaxation after switching off the current.[12] The use of labeled isotopic perchlorate has allowed the evaluation of perchlorate self-diffusion kinetics.[13]

In this context, electrochemically stimulated conformational relaxation (ESCR) is a self-consistent model (with no adjustable parameters)[14−16] that describes and explains the electrochemistry of conducting polymers including both electrochemical and polymeric structural aspects of the materials. Any basic conducting polymer interchanging anions with the electrolyte during the electrochemical reaction will show three main regions where the electric potential controls the composition, structure, or degree of degradation: (i) a region of an intermediate potential, where reverse oxidation/reduction processes occur under diffusion control of the counterions inside the polymer, leading to polymer swelling during oxidation and shrinking during reduction; (ii) a region of more cathodic potentials, where the shrinking material is closed, entrapping a high percentage of counterions, which are slowly expelled by cathodic polarization, inducing a polymer compaction under kinetic control of conformational movements on the chains; and (iii) a region of a polymeric degradation at more anodic potentials than those of region i.

† This paper is dedicated to Prof. Cecilia Sarasola.

* Corresponding author. Phone: (+34) 968325519. Fax: (+34) 968325433. E-mail: toribio.fotero@upct.es.

‡ Present address: Complex Fluids Physics Group, Department of Applied Physics, University of Almeria, 04120 Almeria, Almeria, Spain.

§ Present addresses: Los Alamos National Laboratory, Chemistry Division, Los Alamos, NM 87545, and I'NEST Group, New Technology Research Department, PMUSA, Richmond, VA 23298.

10.1021/jp046051q CCC: $30.25
Published on Web 01/14/2005

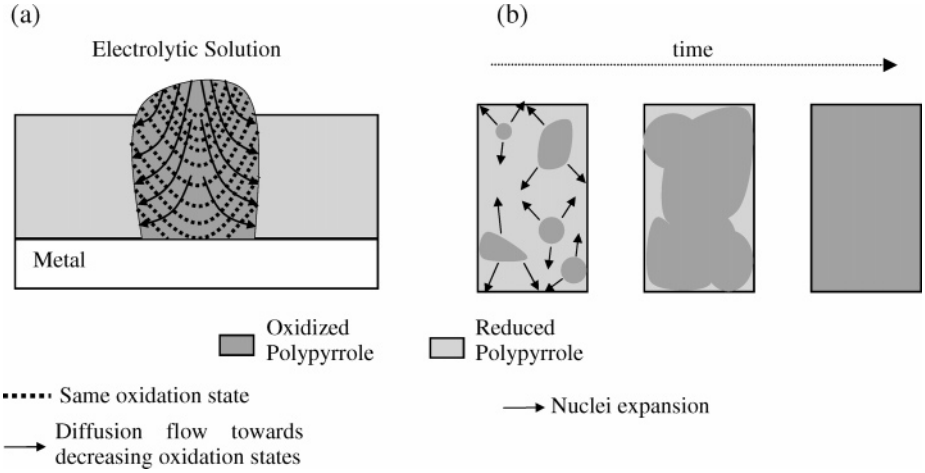

Figure 1. Schematic representation of a nucleation process in polypyrrole: (a) lateral view with representation of the decreasing oxidation density of the material in a nucleus and of the diffusion flow and (b) side up view.

Changes of volume explain the behavior of artificial muscles[17] and the electrochemical behavior of polypyrrole[14−16] and other conducting polymers.[2] The oxidation of a film previously compacted by cathodic polarization starts at well defined points of the polymer/electrolyte interface, where the mobility of the polymeric chains increases with the formation and expansion of nuclei of oxidized material: this is a nucleation process, which can be visualized on electrochromic films.[2,14] This model includes the diffusion of counterions from the bulk of any expanding nuclei, where both counterion content and volume expansion have attained the steady state corresponding to the applied potential, toward the edges of the nuclei (Figure 1), where the oxidation is just starting and the concentration of counterions is very low and the polymer still remains compacted. Under these conditions, the model includes the diffusion coefficient of the counterions between two points of the polymer film, allowing them to be obtained without any additional hypothesis, equivalent circuit, or parameters. This is the aim of this paper, and for comparison, we will make a parallel study and discussion using the Cottrell model, one of the most widely applied models in the literature.

Experimental Section

Chemical. Lithium perchlorate, $LiClO_4$, was from Fluka and potassium nitrate, KNO_3, was from Merck; both of them were A. R. quality and used as received. Pyrrol (Fluka) was distilled under vacuum before use. Water from Milli-Q equipment of 18 MΩ cm was used for the preparation of the solutions. Nitrogen gas of high purity was used for deaeration of the solutions.

Electrochemical Equipment. A PAR/M273A potentiostat−galvanostat, connected to a PC and controlled through M270 electrochemical software, was used. A single compartment electrochemical glass cell was used; the working electrode and counter electrode were platinum sheets with a surface area of 1 and 4 cm^2, respectively, and the reference electrode was of Ag/AgCl (3 M KCl) from Radiometer. All the experiments were carried out at room temperature.

Polypyrrole Electrosynthesis. Polypyrrole films were electrogenerated under galvanostatic conditions by a current density of 1 mA cm^{-2} flowing through a Pt electrode in 50 mM pyrrole and a 0.1 M KNO_3 aqueous solution for 400 s. Figure 2a shows the chronopotentiometric response obtained under those conditions. A 1-μm-thick polypyrrole film, calculated by considering a formation rate of ca. 400 mC cm^{-2} μm^{-1}, as reported by Díaz et al.[18] and Li et al.,[19] was obtained. After electropolymerization,

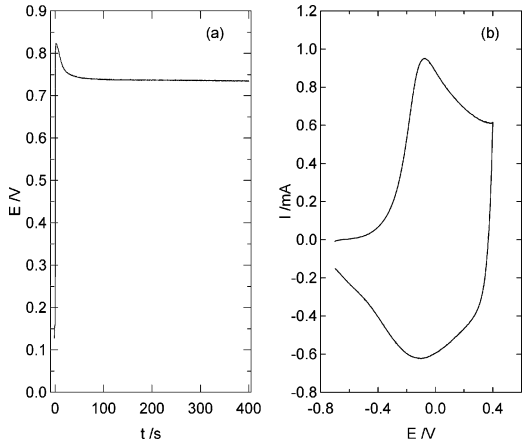

Figure 2. (a) Chronopotentiogram obtained for the galvanostatic electrodeposition of polypyrrole: 1 mA cm^{-2} flowed for 400 s through a 1 cm^2 Pt electrode in a 50 mM pyrrole and 0.1 M KNO_3 aqueous solution at ambient temperature. (b) Control voltammogram obtained under the previously described conditions: after several consecutive voltammograms in 0.1 M $LiClO_4$ aqueous solution between −0.7 and 0.4 V at 20 mV s^{-1} to reach a stationary state and reducing the film by polarization at −0.7V for 60 s.

the coated electrode was rinsed with water and transferred into 0.1 M $LiClO_4$ aqueous solution. The film was submitted to consecutive voltammetric cycles between −0.7 and +0.4 V at 20 mV s^{-1}, until a reproducible voltammogram was obtained. Figure 2b shows the first voltammogram obtained after stabilization, which is similar to those obtained from films synthesized in the presence of perchlorate, confirming the complete replacement of the pristine NO_3^- counterions by ClO_4^-.[13,20]

Theoretical Background. Taking into account that our aim is to explore how best to obtain reliable coefficients inside the swelling/shrinking film of a conducting polymer, we summarize the basic concepts of the Cottrell method, beside those mentioned above for the ESCR models. The fundamental difference between the Cottrell and ESCR models is that the second incorporates structural changes in the polymer in the analysis of the chronoamperograms.

The Cottrell equation describes the evolution of the current, I, along a chronoamperogram, t, as a function of the diffusion coefficient, D:[3]

$$I = \frac{zFAD^{1/2}C}{\pi^{1/2}t^{1/2}} \quad (1)$$

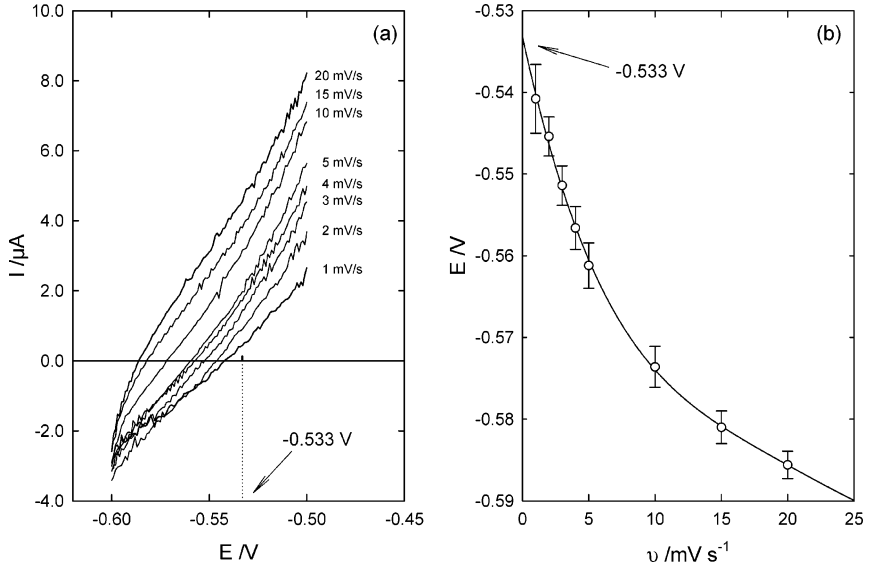

Figure 3. (a) Single voltammogram of the polypyrrole film, according to Figure 2b, between −0.6 and −0.5 V at different scan rates in 0.1 M $LiClO_4$ aqueous solution. (b) Evolution of the crossing potential from cathodic to anodic current, as a function of the sweep rate, υ. By extrapolation at $\upsilon = 0$, an oxidation potential of −0.533 V was obtained.

This equation was obtained under boundary conditions: a planar electrode with a two-dimensional electrode/electrolyte stable interface. A constant concentration, *C*, of the electroactive species is present from the electrode surface to the bulk electrolyte before the potential step. After the potential step, the concentration of the electroactive species drops with time and from the electrode surface in accordance with Fick's second law, and the concentration of the electroactive species is constant in the bulk solution during the potential step *(semi-infinite condition)*. By integration of eq 1 we obtain the evolution of the consumed charge (eq 2) after the potential step:

$$Q = \frac{2zFACD^{1/2}}{\pi^{1/2}} t^{1/2} \tag{2}$$

The result is a linear dependence between the consumed charge, *Q*, and $t^{1/2}$, the slope of which allows us to calculate the diffusion coefficient of the electroactive species through the solution toward the solid electrode. In these equations, *z* is the charge transferred from the polymer by perchlorate ion incorporated during oxidation ($z = 1$), *F* is the Faraday constant (96 485 C mol^{-1}), *A* is the geometric area of the electrode, *C* is the aqueous concentration of the anionic species in mol cm^{-3}, and *D* is the diffusion coefficient in $cm^2\ s^{-1}$.

According to the ESCR model for chronoamperometric experiments, the total charge consumed to oxidize a film and the charge consumed at each time, *t*, after the potential step are related by the expression[14]

$$\ln\left[1 - \frac{Q}{Q_t}\right] = -bt \tag{3}$$

where the diffusion coefficient, *D*, from the already oxidized material toward the oxidation front is included in *b*

$$D = \frac{bh^2}{2} \tag{4}$$

Here, *h* is the thickness of the polymeric film. The constant *b* can be obtained by plotting $\ln(1 - Q/Q_t)$ versus *t*, once the conformational relaxation kinetic control along the chronoamperogram has finished; *Q* is the charge consumed at every time *t* after the potential step (the numerical method of the trapezoid was used for the integration at every *t*); and Q_t is the total charge obtained by integration of the chronoamperogram.

This equation was obtained under the hypothesis that the polymer expands during oxidation, shrinks at the beginning of the reduction (under diffusion kinetic control of the counterion inside the polymer), and then closes, the reduction and compaction continuing under kinetic control of the electrochemically stimulated conformational movements in the polymeric chains. The subsequent oxidation of a reduced and compact polymer film occurs through a nucleation process. Inside each of the expanding nuclei, the oxidation progresses under diffusion control: a concentration gradient appears between those regions of the nuclei where the stationary oxidation state (related to the applied oxidation potential) has already been attained and the edges of the nuclei, where the concentration of counterions is close to zero (see Figure 1). The model includes the same structural effects. Whatever the oxidation state of the polymer, the diffusion processes inside the film, from more oxidized to more reduced parts, are much slower (then kinetic controlling) than diffusion processes through the solution side of the interface.

Results

According to the ESCR model, the polymer begins to swell at the potential where the oxidation starts during a voltammetric experiment involving slow potential sweeps. To ascertain this starting potential of the oxidation process, so that it might be taken as a reference to study the compaction/swelling processes, single voltammograms were performed between −0.6 and −0.5 V at different scan rates. This potential window was selected because it includes the crossing point from cathodic to anodic currents. Figure 3a represents one voltammogram from each of the studied sweeps rates: 1, 2, 3, 4, 5, 10, 15, and 20 mV s^{-1}. The procedure was repeated five times, starting with the slowest and finishing with the fastest of the studied sweep rates, every time. The crossing potential (beginning of oxidation) was measured from each of the five voltammograms obtained at the same scan rate, and the average and standard deviation were calculated. The results obtained for the different scan rates can be observed in Figure 3b. By extrapolation to zero scan rate, the potential for the beginning of the oxidation under stationary conditions (−0.533 V versus Ag/AgCl) was obtained.

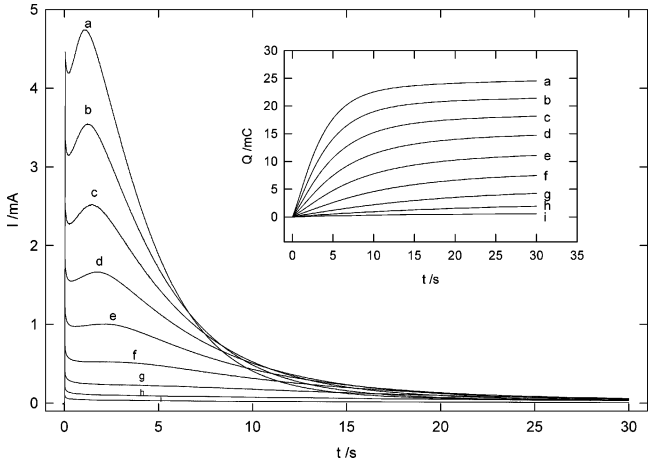

Figure 4. Chronoamperograms obtained when the polypyrrole film was submitted to anodic potential pulses. The initial potential was −0.533 V (maintained for 30 s) followed by a potential step to (a) +0.367 V (ΔE = 900mV), (b) +0.267 V (ΔE = 800 mV), (c) +0.167 V (ΔE = 700 mV), (d) +0.067 V (ΔE = 600 mV), (e) −0.033 V (ΔE = 500 mV), (f) −0.133 V (ΔE = 400 mV), (g) −0.233 V (ΔE = 300 mV), (h) −0.333 V (ΔE = 200 mV), and (i) −0.433 V (ΔE = 100 mV) in 0.1 M $LiClO_4$ aqueous solution, where ΔE is the potential step. The inset corresponds to the integrated charge during the chronoamperogram, to obtain the respective chronocoulograms.

Depending on the interactions that take place among the reduced polymer, the solvent, and the counterions, we should expect the closing potential of polypyrrole to be around the potential where oxidation starts. At the closing potential, which is defined according to the progressive shrinking of the oxidized and swollen polymer during reduction under diffusion control, pores inside the partially oxidized material are thinner than the counterion diameter, which forces the polymeric chains to open up a way toward the solution: the reduction continues under conformational relaxation and migration control. At the closing potential, the polymer still remains partially oxidized. Under this hypothesis, any polarizations at more negative potentials will promote greater reduction and compaction of the polymeric structure by expulsion of counterions and destruction of the concomitant free volume. Any subsequent oxidation of the material requires time (under potentiostatic conditions) for the compacted structure to open up, starting at those points of the polymer/electrolyte interface with greatest chain mobility, which gives a well-defined nucleation maximum to the chronoamperograms.[2,14] To check the presence or not of compaction at the above oxidation potential obtained by extrapolation from kinetic conditions, a series of stationary experiments was performed involving potential steps from −0.533 V, maintained for 30 s every time, to different oxidation potentials. The chronoamperograms obtained are depicted in Figure 4, each showing the maximum characteristic of the relaxation−nucleation processes, which demonstrates the presence of compaction at −0.533 V. So, the oxidation potential obtained by dynamic experiments is more cathodic than the closing potential obtained from chronoamperometric experiments, as was previously shown for thick films.[21] Under these conditions for the chronoamperometric experiments, the kinetic diffusion control of the process only occurs after the inflection point following the maximum. This region will be used for obtaining D when nucleation processes are present.

To detect the lowest potential of polarization, allowing subsequent oxidation under diffusion kinetic control (without any maxima or inflection point on the chronoamperogram), a second experimental series was performed involving potential steps to +0.367 V, exploring different initial potentials, which were maintained for 30 s every time. Figure 5 depicts the chronoamperograms obtained. The results obtained from −0.533, −0.433, and −0.333 V show a maximum, indicating the consecutive presence of relaxation−nucleation and diffusion-controlling kinetic processes, during the time represented by the chronoamperogram. Experiments performed starting from more positive potentials (−0.233, −0.133, −0.033, 0.067, and 0.167 V) show monotonically decaying currents throughout the oxidation time with diffusion control. From these experiments, with soft polymer structure, both models should be expected to give similar D values.

Considering these results, another series of potential steps was planned under diffusion control: the polymer was polarized

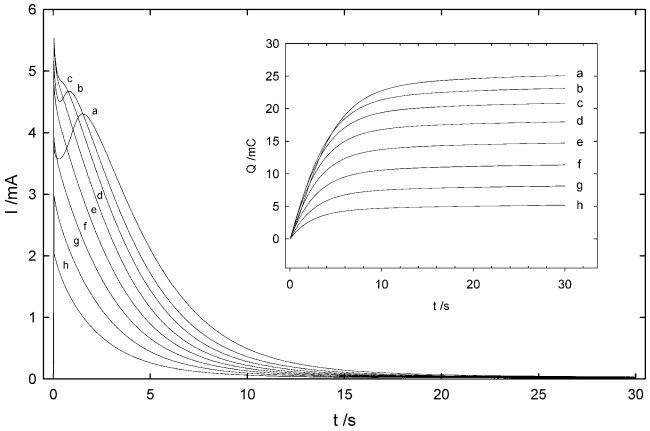

Figure 5. Chronoamperograms obtained from different initial potentials up to +0.367 V with initial potentials of (a) −0.533 V (ΔE = 900 mV), (b) −0.433 V (ΔE = 800 mV), (c) −0.333 V (ΔE = 700 mV), (d) −0.233 V (ΔE = 600 mV), (e) −0.133 V (ΔE = 500 mV), (f) −0.033 V (ΔE = 400 mV), (g) +0.067 V (ΔE = 300 mV), and (h) +0.167 V (ΔE = 200 mV), where ΔE is the potential step, in 0.1 M $LiClO_4$ aqueous solution. The inset corresponds to the integrated charge during the chronoamperogram to obtain the respective chronocoulograms.

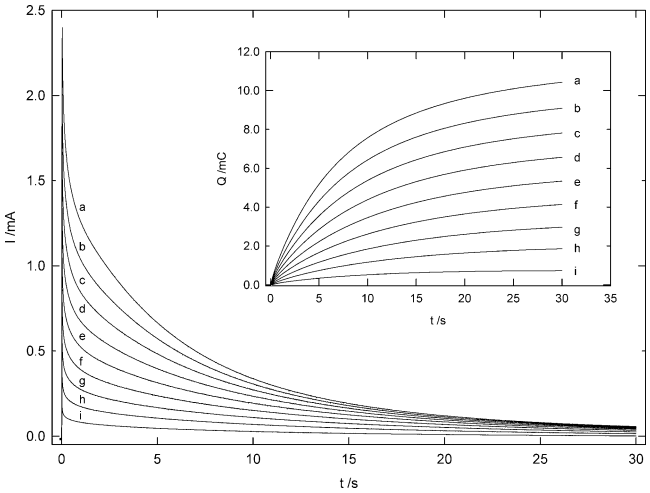

Figure 6. Chronoamperograms obtained in 0.1 M $LiClO_4$ aqueous solution by potential pulses from −0.233 V (the polymer is not compacted at this potential) to different anodic potentials: (a) +0.217 V (ΔE = 450 mV), (b) +0.167 V (ΔE = 400 mV), (c) +0.117 V (ΔE = 350 mV), (d) +0.067 V (ΔE = 300 mV), (e) +0.017 V (ΔE = 250 mV), (f) −0.033 V (ΔE = 200 mV), (g) −0.083 V (ΔE = 150 mV), (h) −0.133 V (ΔE = 100 mV), and (i) −0.183 V (ΔE = 50 mV), where ΔE represents the potential step. The inset corresponds to the integrated charge, during the chronoamperogram, to obtain the respective chronocoulograms.

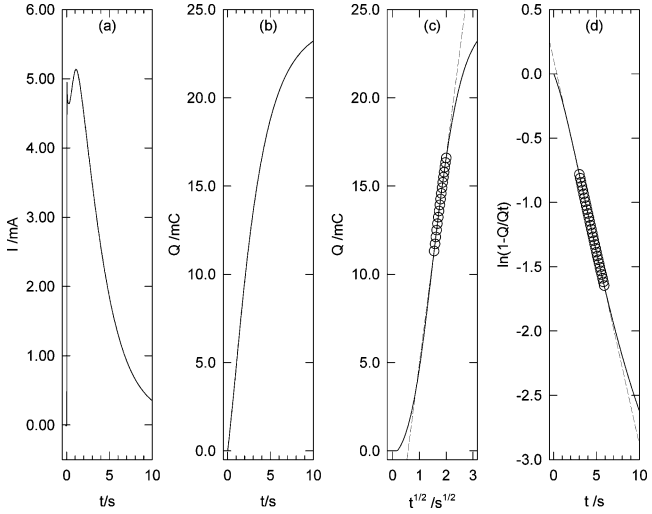

Figure 7. Treatment of the experimental results to obtain the diffusion coefficients. (a) Experimental chronoamperogram, (b) chronocoulogram obtained by integration of the chronoamperogram of part a, (c) Cottrell relationships, and (d) ESCR model. The shown plots are related to the potential step from −0.533 V, kept for 60 s, to +0.367 V in 0.1 M $LiClO_4$ aqueous solution. A similar treatment was performed on each experimental chronoamperogram.

at −0.233 V for 30 s, in which case it was oxidized at different anodic potentials, as Figure 6 shows.

Discussion

Experimental chronoamperograms from Figure 4 show a maximum that agrees with that observation in the ESCR model[15,16] and reflects conformational relaxation of the polymeric chains on specific nuclei at the polymer/electrolyte interface (where the mobility of the chains is greater) in order to create a free volume that allows penetration of the counterions. The oxidized nuclei expand (the current rises on the chronoamperogram) and coalescence (the current goes through a maximum) during polarization. The inflection point after the maximum indicates the end of the coalescence processes and the beginning of the completion of oxidation under diffusion control. To compare results obtained from both the Cottrell and ESCR model, only the part of the chronoamperograms where diffusion prevails was used to calculate the diffusion coefficients. The inset of Figure 4 shows the integrated chronoamperograms (Q vs t), the chronocoulograms.

Figure 7 shows one of the experimental chronoamperograms (i vs t), the concomitant integrated chronocoulograms (Q vs t), and their representation according to the Cottrell model (Q vs $t^{1/2}$, eq 2) or according to the conformational relaxation model [$\ln(1 - Q/Q_t)$ vs t, eq 3]. Diffusion coefficients were obtained from the last two plots. When the initial potential was kept constant at −0.533 V, changing the anodic potential (Figure 4), increasing diffusion coefficients were obtained for increasing anodic potential limits for both models (Figure 8). In a previous work,[14] the ESCR model showed an increasing linear relationship between the oxidation degree of the film and the diffusion coefficient obtained by potential steps in a shorter potential range. In both cases, we start from the same compaction state of the film and, by increasing anodic overpotentials, promote rising oxidation/swelling rates and easier diffusion processes. These results corroborate[19] the faster electrochemical stimulation of the conformational movements of the polymeric chains, promoting the opening, oxidation, and swelling of the film; the greater the potential step, the faster the process. The diffusion

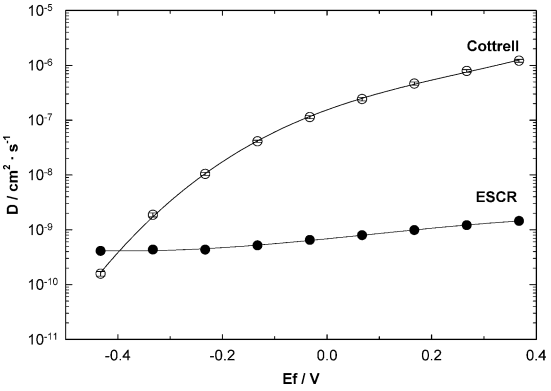

Figure 8. Semilogarithmic evolution of D as a function of the final potential, Ef, with initial potential of −0.533 V (Figure 4). The error bars average five experiments, and their size depicts the standard deviations.

coefficients obtained from the Cottrell expression were only similar to those obtained from the ESCR model when the polymer was submitted to potential steps lower than 100 mV. This may be attributed to the small potential steps, which induce slow oxidation (and diffusion) processes, minimizing structural effects. As the potential steps increased, so the differences in the diffusion coefficient became greater, until the values were 4 orders of magnitude greater in the Cottrell model than in the ESCR model. The Cottrell coefficients obtained agree with those reported by Pickup et al,[11] while those obtained with the ESCR model are closer to those obtained by the same authors using impedance measurements.[10] From our point of view, these discrepancies arise because the Cottrell equation does not adequately describe the transport of ions within conducting polymers undergoing structural transformation. Since these structural changes depend on the amplitude of the potential step, both models converge when the structural changes disappear for small potential steps. Table 1 presents the diffusion coefficients obtained with the different experimental methods.

In summary, two main facts can be underlined: first, the diffusion coefficients obtained from chronoamperometric measurements when the initial potential and the polarization time at this initial potential are maintained constant are a function of the oxidation potential (the potential step); and second, the diffusion coefficients obtained with the ESCR model are several orders of magnitude lower than those obtained with the Cottrell method and closer to those expected for a cross-linked polymer.

Our question now concerned the influence of the initial potential and how the initial state of polymeric compaction or swelling influences the diffusion coefficient. We started with a potential step from −0.533 V, kept for 30 s, to +0.367 V, to attain a diffusion coefficient as previously shown in Figure 8. Then, different initial potentials, maintained every time for 30 s and stepped to the same final potential of +0.367 V, were performed (Figure 5). Figure 9 shows the diffusion coefficients obtained. Once again, the Cottrell expression did not match the expected physics. When we started with increasing open and swollen initial states from rising initial potentials (increasing coefficients are to be expected, despite the decreasing potential gradients), the Cottrell treatment produced ever decreasing (up to 20 times lower) diffusion coefficients. Increasing values were obtained with the ESCR model, all in the range from 1.2×10^{-9} to 1.8×10^{-9} $cm^2\ s^{-1}$, which is much more consistent with that expected for an open gel structure. Summarizing, Figure 9 reflects the influence of two effects: the initial increasing swelling state of the polymer, which should promote a rise in D with increasing initial potentials, and the decreasing

TABLE 1: Diffusion Coefficients Obtained Using Different Experimental Methodologies and Different Theoretical Models

polymeric matrix	doping soln (electrolyte/solvent)	D/cm^2 s^{-1}	technique	ref
poly(pyrrole−ClO_4^-−CH_3CN)	ClO_4^-/PC[a]	$(0.5-1.0) \times 10^{-12}$	impedance	9
poly(pyrrole−TBAP[b]−PC)	ClO_4^-/H_2O	4.2×10^{-8}	isotopic labeled	13
poly(pyrrole−TBAP−PC)	ClO_4^-/CH_3CN	3.6×10^{-10}	isotopic labeled	13
poly(pyrrole−TBAP−PC)	ClO_4^-/PC	3.0×10^{-13}	isotopic labeled	13
poly(pyrrole−ClO_4^-−H_2O)	ClO_4^-/H_2O	3.7×10^{-8}	impedance	10
poly(pyrrole−NO_3^-−H_2O)	ClO_4^-/H_2O	$\approx 1 \times 10^{-6}$ (oxidized) $\approx 4 \times 10^{-10}$ (reduced)	Cottrell	this work
poly(pyrrole−NO_3^-−H_2O)	ClO_4^-/H_2O	$\approx 1.5 \times 10^{-9}$ (oxidized) $\approx 4 \times 10^{-10}$ (reduced)	ESCR	this work

[a] PC: propylene carbonate. [b] TBAP: perchlorate tetrabutylammonium.

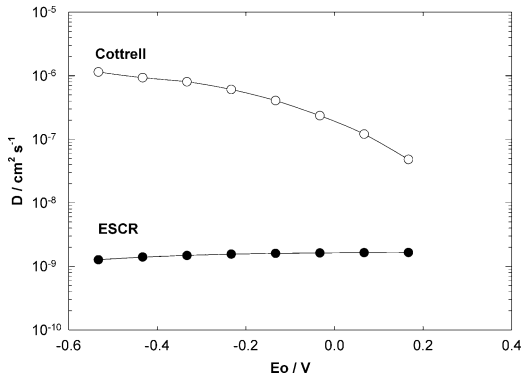

Figure 9. Semilogarithmic evolution of D as a function of the initial potential, when final potential was +0.367 V (obtained from chronoamperograms shown in Figure 5).

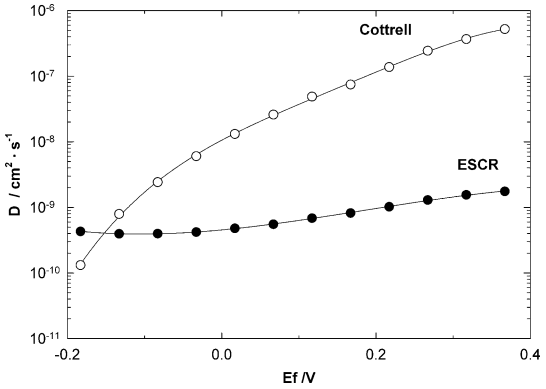

Figure 10. Semilogarithmic evolution of D as a function of the initial potential using monotonically decreasing chronoamperograms from Figure 6.

experimental potential gradient, which would be expected to induce a drop in D due to decreasing swelling rates during the oxidation process. In Figure 10 the same features are depicted, considering pure diffusional chronoamperograms (Figure 6), and the diffusion coefficient ranges between 0.4×10^{-9} and 2×10^{-9} cm^2 s^{-1}.

To differentiate between these effects (initial state and potential gradient), potential steps were performed using constant potential gradients of 100, 200, 300, 400, 500, 600, 700, 800, and 900 mV, starting from different initial potentials (Figure 11). As expected from the fact that the oxidations started from increasing oxidation states (i.e. from increasing degrees of swelling of the polymer), increasing diffusion coefficients were obtained. The diffusion coefficient obtained from a swollen film at −0.100 V was five times greater than that from a compacted film at −0.533 V.

Taking into account eq 4, increasing diffusion coefficients might be expected to be correlated with an increasing volume

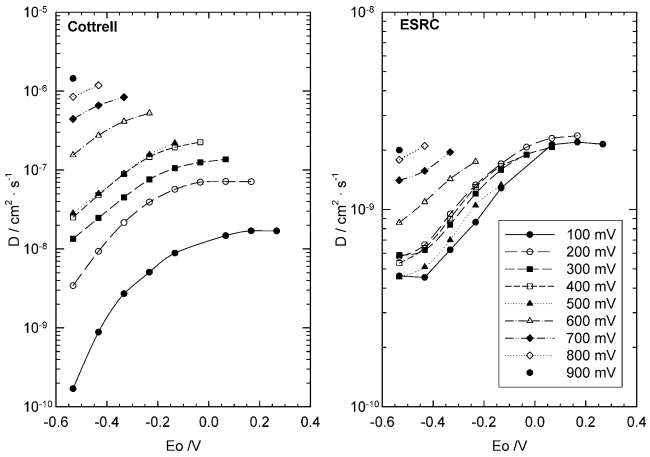

Figure 11. Semilogarithmic evolution of D as a function of the initial potential using a constant potential step and for different potential steps: Cottrell and the ESCR models.

and thickness of the polymer film if we consider that up to 50% of the thickness change (h)[22] in eq 3 should give a variation of 2.25 times in the diffusion coefficient, which is far from the 5-fold change found, regardless of the range of the studied potential step. These results indicate that, besides the increase in the film thickness during oxidation, we must take into consideration that the swelling process also changes the rheological properties (i.e. viscosity) of the material.

So from this study we can state that by extrapolation of the voltammetric measurements at different sweep rates, the oxidation of the studied polypyrrole film was seen to start at −0.533 V. Nevertheless, potentiostatic experiments demonstrated that the polymer could be reduced and compacted by polarization at cathodic potentials equal or lower than −0.333 V. According to the ESCR model, this seems a paradox: the polymer is reduced and compacted in aqueous solution at a stationary potential more positive than the oxidation potential observed by extrapolation to a zero sweep rate using a dynamic voltammetric method. In the case of conducting polymers, due to the slow structural effects of the electrochemical reactions on the chain conformations, dynamic experiments lead to different conclusions from those reached in stationary experiments. Under dynamic conditions, it is difficult to attain polymeric compaction during cathodic potential sweeps, while polymeric oxidation on the subsequent anodic sweep occurs at low potentials, closer to those of a free chain polymer in solution. Under stationary polarization, reduction and compaction are greatest: the subsequent oxidation involves structural control of nucleated processes, such as that observed in the chronoamperograms.

As regards determining the diffusion coefficient, the hypothesis of the Cottrell model cannot be applied to the study of the oxidation/reduction processes of conducting polymers, where

the state of compaction/swelling changes as a function of the applied potential. The ESCR model takes into consideration these changes, together with diffusion processes inside the polymer, between those regions where the steady state of the polymer oxidation induced by the applied potential has been attained and the regions where the oxidation is still in progress. In this way the ESCR model allows the swelling degree, induced by the applied potential, to be correlated with the attained diffusion coefficient. Thus, increasing values of D were obtained when, starting from the same cathodic potential of compaction, potential steps to higher anodic potentials were applied. These results were attributed to the faster swelling processes occurring under increasing potential gradients. The faster increase in the film thickness and the faster decrease in viscosity seem to be responsible for the increasing D values.

When the potential steps were performed starting from increasing initial potentials (increasing oxidation states and swelling degrees of the film) to reach the same final potential, increasing D values were obtained. This increase occurred despite the decrease in the potential gradient, which, as stated in the previous conclusion, promotes a rapid decrease in D.

Both models overlapped when the structural effects were minimized by starting from an open structure and applying potential gradients lower than 100 mV. Neither the Cottrell nor the ESCR model takes into account the rheological changes induced by redox processes at the different potentials.

Acknowledgment. The authors wish thanks Kraft Foods Inc. (NanoTeK) for the financial support which enabled us to carry out this work.

References and Notes

(1) Otero, T. F.; Bengoechea, M. *Langmuir* **1999**, *15*, 1323−1327.
(2) Otero, T. F.; Boyano, I. *ChemPhysChem* **2003**, *4*, 868−872.
(3) Bard, A.; Faulkner, L. R. *Electrochemical Methods. Fundamentals and Applications*, 2nd ed.; John Wiley & Son, Inc.: New York, 2001; pp 161−164.
(4) Macdonald, J. R., Ed. *Impedance Spectroscopy*; John Wiley & Son: New York, 1987.
(5) Mostany, J.; Scharifker, B. R. *Synth. Met.* **1997**, *87*, 179−185.
(6) Levi, M. D.; Aurbach, D. *J. Electrochem. Soc.* **2002**, *149*, E215−E221.
(7) García-Belmonte, G. *Electrochem. Commun.* **2003**, *5*, 236−240.
(8) Penner, R. M.; Martin, C. R. *J. Phys. Chem.* **1989**, *93*, 984−989.
(9) García-Belmonte, G.; Bisquert, J. *Electrochim. Acta* **2002**, *47*, 4263−4272.
(10) Ren, X.; Pickup, P. G. *J. Phys. Chem.* **1993**, *97*, 5356−5362.
(11) Paulse, C. D.; Pickup, P. G. *J. Phys. Chem.* **1988**, *92*, 7002−7006.
(12) Penner, R. M.; Van Dike, L. S.; Martin, C. R. *J. Phys. Chem.* **1988**, *92*, 5274−5282.
(13) Schlenoff, J. B.; Chien, C. W. *J. Am. Chem. Soc.* **1987**, *109*, 6269−6274.
(14) Otero, T. F.; Grande, H.; Rodríguez, J. *J. Phys. Chem. B* **1997**, *101*, 3688−3697.
(15) Otero, T. F.; Grande, H.; Rodríguez, J. *J. Electroanal. Chem.* **1995**, *394*, 211−216.
(16) Otero, T. F.; Grande, H.; Rodríguez, J. *Electrochim. Acta* **1996**, *41*, 1863−1869.
(17) Otero, T. F.; Cortes, M. T. *Adv. Mater.* **2003**, *15*, 279−282.
(18) Díaz, A. F.; Castillo, J. I.; Logan, J. A.; Lee, W. *J. Electroanal. Chem.* **1981**, *129*, 115−132.
(19) Li, Y.; Qian, R. *Electrochim. Acta* **2000**, *45*, 1727−1731.
(20) Curtin, L. S.; Komplin, G. C.; Pietro, W. J. *J. Phys. Chem.* **1988**, *92*, 12−13.
(21) Otero T. F.; Ariza, M. J. *J. Phys. Chem. B* **2003**, *107*, 13954−13961.
(22) Otero, T. F. In *Handbook of Organic Conductive Molecules and Polymers*; Nalwa, H. S., Ed.; John Wiley & Sons: Chichester, 1997; Vol. 4, pp 522−523.